

## Effects of Lower Limb Torsion on Ankle Kinematic Data During Gait Analysis

†Kit M. Song, M.D., \*M. Cecilia Concha, B.S., and ‡Nasreen F. Haideri, M. Engr.

*Study conducted at the Texas Scottish Rite Hospital for Children, Dallas, Texas, U.S.A.*

**Summary:** VICON Clinical Manager software is widely used for gait analysis and has four methods for computing ankle plantarflexion–dorsiflexion motion and transverse plane ankle rotation profiles. The authors evaluated 14 subjects with a diagnosis of spastic cerebral palsy and tibial torsion ranging from 39° internal torsion to 90° external torsion, using the four different processing methods. It was found that clinically measured tibial torsion >20° external or >15° internal led to sig-

nificant differences in the calculated ankle plantarflexion–dorsiflexion and transverse plane ankle rotation measurements between the four methods. Pearson correlations indicated that these differences increased with increasing external or internal tibial torsion. The variability was enough to affect conclusions of published articles and clinical decision making. **Key Words:** Ankle motion—Ankle rotation—Gait analysis—Tibial torsion.

Three-dimensional kinematic and kinetic gait analyses are being increasingly used to characterize motion and to make recommendations for the treatment of pathologic gait (5–7,13,19–21). The data generated by gait analysis are interpreted through a mathematical model. Although it is not necessary to have a comprehensive understanding of the mathematical formula used to generate three-dimensional data, it is important for accurate interpretation of that data to have a complete understanding of the model and the assumptions inherent to it.

Most gait analysis systems use surface landmarks to create local embedded reference frames to track limb segment movement. Joint center locations and anatomic axes are calculated from the data derived and from relationships defined by the anatomic models incorporated in the gait analysis software. The calculated rotations about the anatomic axes are then output. The calculated movement of limb segments about joint axes is dependent on the mathematical and anatomic modeling assumptions inherent in the software. Kadaba et al. (9) developed a model that has been widely incorporated into clinical and research applications (3,4) as well as commercially available software, including VICON Clinical Manager

(VCM) analysis software (Oxford Metrics Ltd., Oxford) (12). Our laboratory and approximately 45 centers in the United States use the VCM analysis software for clinical and research applications. Early studies, including Kadaba et al.'s, focused on the characterization of gait for normal subjects. In the evaluation of normal gait, subtle differences in modeling techniques are not appreciated in the resulting joint motion. Many centers, however, are involved in the treatment of patients with moderate to severe musculoskeletal or neuromuscular abnormalities. These require special considerations in marker placement and in data processing.

It is the purpose of this paper to examine the effect that differing modeling assumptions have on calculated values of sagittal plane ankle motion in children with cerebral palsy with a range of torsional abnormalities of the tibia.

### METHODS

We retrospectively reviewed the gait studies of 14 children who had been previously tested in our laboratory and whose clinically measured torsional profile represented a broad range of internal to external torsion. The age, clinically measured tibial torsion, and ambulatory status for each child are shown in Table 1. The clinical measurement of tibial torsion was performed by placing the patient in a sitting position with the hips and knees flexed to 90° and the patella and tibial tubercle pointing forward (18), or by placing the patient in a prone position with the hips in full extension and the knees flexed to 90°. The malleoli were palpated and the line joining them (bimalleolar axis) was estimated. The degree of tibial

Address correspondence and reprint requests to Kit M. Song, M.D., Children's Hospital and Regional Medical Center of Seattle, 4800 Sand Point Way NE, P.O. Box 5371/CH-59, Seattle, WA 98105, U.S.A. (e-mail: ksong@chmc.org).

From \*Shriners Hospitals for Children, Erie, Pennsylvania; †Children's Hospital and Medical Center, Seattle, Washington; and ‡Texas Scottish Rite Hospital for Children, Dallas, Texas, U.S.A.

TABLE 1. Demographics

Subject	Age	Tibial torsion	Diagnosis	Ambulatory status
1	17 + 8	R, 90° ext.	Spastic diplegia	Use of bilateral Lofstrand crutches
2	10 + 1	R, 70° ext.	Spastic diplegia	Independent ambulator
3	11 + 8	L, 60° ext.	Spastic diplegia	Use of bilateral Lofstrand crutches
4	13 + 1	R, 56° ext.	Spastic diplegia	Independent ambulator
5	14 + 8	R, 48° ext.	Spastic diplegia, talipes equinovarus	Independent ambulator
6	17 + 5	R, 40° ext. L, 30° ext.	Spastic triplegia	Independent ambulator
7	15 + 3	L, 25° ext.	Spastic quadriplegia	Use of bilateral Lofstrand crutches
8	14 + 11	L, 19° ext.	Spastic diplegia	Independent ambulator
9	13 + 5	L, 12° ext.	L: hemiplegia, status post astrocytoma resection R: hemisphere	Independent ambulator
10	13 + 5	R, 7° ext. L, 12° int.	Spastic diplegia	Use of bilateral ankle-foot orthoses
11	18 + 7	R, 0° neut. L, 5° int.	Spastic triplegia	Independent ambulator
12	14	R, 22° int. L, 26° int.	Femoral anteversion, internal tibial torsion	Independent ambulator
13	4	R, 30° int.	Left spastic hemiplegia	Use of left ankle-foot orthosis
14	14 + 11	L, 35° int. R, 39° int.	Spastic diplegia	Use of left Lofstrand crutch

torsion was measured using a goniometer as the angle between the visualized bimalleolar axis and the femoral epicondylar axis.

Each child was evaluated with a six-camera VICON system using 13 reflective tracking markers as described by the VCM software manual (12). Markers were placed midway between the posterior superior iliac spines, bilaterally on the anterior superior iliac spines, on the most prominent point of the lateral femoral epicondyle, on a laterally placed midthigh wand in a line between the greater trochanter and the lateral femoral epicondyle, on the most prominent point of the lateral malleolus, on a lateral shank wand visually aligned parallel to the bimalleolar axis, and on the midfoot, slightly proximal to the second metatarsal head. These 13 markers were tracked during a static data trial and during “dynamic” data trials to calculate virtual joint center locations as described by Davis et al. (4).

VCM software was used to process each data trial. This software has the option of using a spring clamp with three reflective markers on the tip of three orthogonal wands called a knee alignment device (KAD) on each knee to bridge the medial and lateral femoral epicondyles during a static data trial. The KAD defines a “preferred” frontal plane for the thigh segment using a virtual hip and knee joint center and a virtual point at the base of the KAD. This in turn establishes an anatomically correct transverse plane alignment of the knee flexion–extension axis. Correction factors or static “rotation offset” angles are then calculated for the thigh and shank segments. The thigh rotation offset angle was applied to the dynamic data trials to realign the thigh segment’s frontal plane based on tracking markers, with the anatomically correct frontal plane derived from the use of the KAD. For the purposes of this study, all patient data collection was performed with the KAD option and the thigh rotation offset corrections to the local embedded reference frames

for bilateral thigh segments. This step was maintained for the processing of the four methods.

In the same fashion as the thigh rotation offset angle, the shank rotation offset angle can be calculated from the use of the KAD during a static data capture. The “preferred” frontal plane of the shank segment varies depending on the inclusion or exclusion of the clinically measured tibial torsion value.

VCM software has four available methods for processing the relative position of the shank and foot segments (Figs. 1–4). Each of these methods results in a different shank rotation offset. This leads to a change in the transverse plane orientation of the ankle plantarflexion–dorsiflexion (PF/DF) axis and the location of the calculated virtual ankle joint center. This alters the kinematic calculations for the ankle complex (sagittal ankle PF/DF and transverse plane ankle rotation, referred as foot rotation in VCM).

Each child had three walking trials. Several representative gait cycles from each trial were recorded. A single gait cycle within one standard deviation of the ensemble average for each subject’s data was selected for this evaluation. To illustrate differences between the processing methods rather than deviations between cycles, the single representative cycle was used with each of the four processing methods. We calculated ankle PF/DF motion and transverse plane ankle rotation using each of the four methods at seven key points in the gait cycle: initial foot contact, opposite foot off, midstance, opposite foot contact, foot off, midswing, and terminal foot contact. We then calculated the average and standard deviation for these movements. Pearson correlation coefficients were calculated for the standard deviation of the ankle range of motion at these seven specific key points versus the value of clinically measured tibial torsion to see whether the variability across the four methods changed as the tibial torsion increased. Absolute differ-

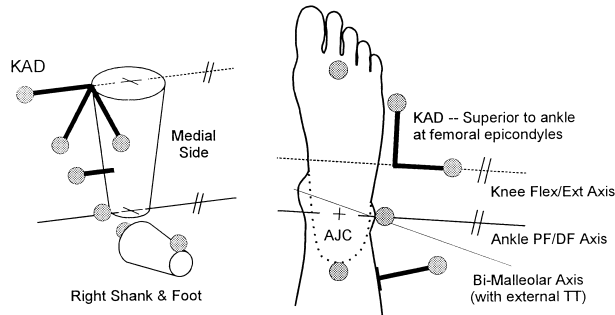


**FIG. 1.** Method 1: ankle plantarflexion–dorsiflexion (PF/DF) axis is parallel to knee flexion/external axis. The tibial torsion is set to 0. The local embedded reference frames for both the thigh and the shank segments are realigned (via rotation offset angles) to reflect the preferred frontal plane predetermined by the knee alignment device placement. Therefore, the frontal planes for the thigh and shank segments are parallel. The virtual ankle joint center (AJC) is calculated to lie on the axis that contains the lateral malleolus marker (parallel to the femoral epicondylar axis) and is displaced medially half the distance of measured ankle width. In the case of external tibial torsion (as shown), the AJC is calculated posterior and lateral to the desired location (toward the heel) and the ankle PF/DF axis is misaligned. In the case of internal tibial torsion, the error in AJC calculation is in the anterior direction (closer to the toes) as well as a misaligned ankle PF/DF axis. Transverse plane ankle rotation (about the long axis of the shank) is defined as the angle between the sagittal plane projection of a vector defining the long axis of the foot and the perpendicular axis relative to the frontal plane of both the shank segment and the parallel (//) thigh segment.

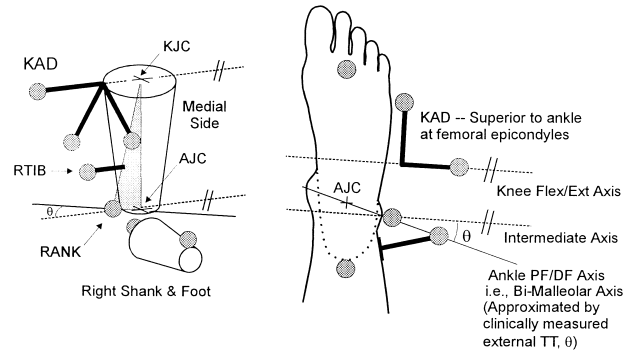


**FIG. 3.** Method 3: ankle plantarflexion–dorsiflexion (PF/DF) axis is rotated to reflect technically measured tibial torsion. The tibial torsion is set to 0. The static calibration trial is processed, then the shank rotation offset angle is set to 0 before the processing of the dynamic trials. The calculated ankle PF/DF axis is now corrected to reflect the technically measured tibial torsion, which lies on a plane containing the knee joint center (KJC), lateral shank wand marker (RTIB), and ankle joint center (AJC). The AJC is calculated to lie on the corrected ankle PF/DF axis reflecting the RTIB marker placement and is displaced medially half the distance of the measured ankle width. Transverse plane ankle rotation is calculated as in methods 1 and 2. Therefore, if the clinical measure of tibial torsion and the technical approximation of tibial torsion (i.e., accurate RTIB marker placement) are similar, methods 2 and 3 yield similar results for the calculated ankle PF/DF axis, the AJC, and the transverse plane ankle rotation. In addition, if the clinically measured tibial torsion equals 0 and the technical approximation of tibial torsion is accurate, methods 1, 2, and 3 will yield similar results.

ences between each of the four methods were also calculated at each of the seven key points in the gait cycle for ankle PF/DF and transverse plane ankle rotation. A maximum difference for calculated ankle PF/DF between each of the four methods over the entire gait cycle was also determined.

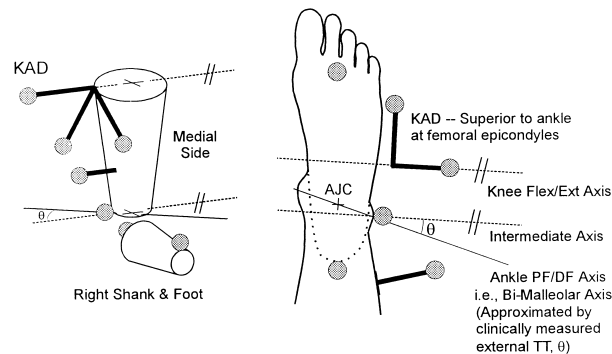


**FIG. 2.** Method 2: ankle plantarflexion–dorsiflexion (PF/DF) axis is rotated to reflect clinically measured tibial torsion. The clinical measure of tibial torsion ( $\theta$ ) is entered. The calculated shank rotation offset angle reflects an adjustment for the value of tibial torsion. The calculated ankle PF/DF axis is corrected to reflect a more accurate estimation of the anatomic bimalleolar axis. The calculated ankle joint center (AJC) lies on the corrected axis containing the lateral malleolus marker and is displaced medially half the distance of measured ankle width, reflecting a more anatomically correct location for AJC. Transverse plane ankle rotation is calculated as in method 1; however, the frontal plane of the shank segment differs by the value of tibial torsion. Therefore, if the value of clinically measured tibial torsion equals 0, then method 1 and method 2 are equal.

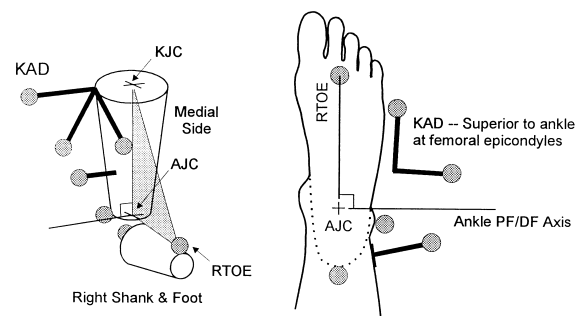


**FIG. 4.** Method 4: ankle plantarflexion–dorsiflexion (PF/DF) axis is perpendicular to knee-ankle-toe plane (KJC-AJC-RTOE). The clinical measure of tibial torsion ( $\theta$ ) is entered. The calculated shank rotation offset angle reflects an adjustment for the value of tibial torsion. The ankle joint center (AJC) is calculated as in method 2. Once the AJC is derived, a new “foot-based” ankle PF/DF axis is calculated to lie perpendicular to the plane containing the knee joint center (KJC), the AJC, and the right toe (RTOE) marker. Transverse plane ankle rotation or the “shank-based” ankle rotation is calculated as in method 1, in which the frontal plane of the shank segment is assumed to be parallel to the thigh segment. Therefore, extreme profiles of external or internal tibial torsion will not affect the “shank-based” ankle rotation measurement.

**RESULTS**

As clinically measured tibial torsion increased either externally or internally, the variability of the calculated ankle PF/DF between the four methods also increased. When the clinically measured tibial torsion ranged from 19° external to 12° internal, the average difference for the calculated ankle PF/DF between each of the four

methods at all points of the gait cycle was 5° or less. When the tibial torsion was >30° external or 39° internal, >10° of variability in the calculated ankle PF/DF for the four methods was found. This was reflected by an increase in the standard deviation between the calculated ankle PF/DF for the four methods at the seven key points of the gait cycle (Fig. 5).

An example of the calculated differences is shown in Figure 6 for a child with extreme bilateral femoral anteversion and 90° external tibial torsion. In method 1, the ankle PF/DF motion has a range of neutral to 8° dorsiflexion, and transverse plane ankle rotation is approximately 30° external. Method 2 has a range of 57° plantarflexion to 7° dorsiflexion, and transverse plane ankle rotation is 55°–65° internal. Method 3 plots very slight plantarflexion and dorsiflexion with transverse plane ankle rotation having a more neutral position. Method 4 documents motion of ankle PF/DF from 20° plantarflexion to 3° dorsiflexion with a transverse plane ankle rotation of approximately 25°–30° external rotation.

Standard deviations for transverse plane ankle rotation also increased with increasing values of tibial torsion, but the effects were more pronounced and were seen with even small degrees of torsion (Fig. 7). Pearson correlation analysis of ankle PF/DF and transverse plane ankle rotation with the standard deviations generated by the four methods showed a linear relationship of increased variation with increased values of external tibial torsion and a strong correlation with increased internal tibial torsion (Table 2).

DISCUSSION

Three-dimensional motion tracking systems have been increasingly used as a tool for making clinical diagnoses and recommendations for treatment of gait abnormalities and for measuring the outcomes of clinical treatment. Several authors have described small changes in ankle kinematics to be clinically significant (14,17,22). Rose et al. (14) reported a mean increase of 8° dorsiflexion at

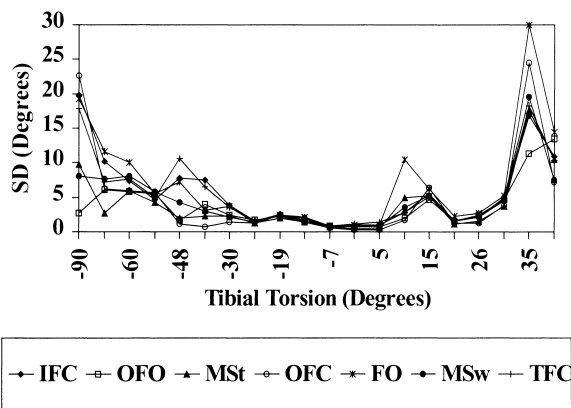


FIG. 5. Standard deviation of methods 1 to 4 for the ankle plantarflexion–dorsiflexion motion versus the tibial torsion value at seven key points in the gait cycle: initial foot contact (IFC), opposite foot off (OFO), midstance (MSt), opposite foot contact (OFC), foot off (FO), midswing (MSw), and terminal foot contact (TFC).

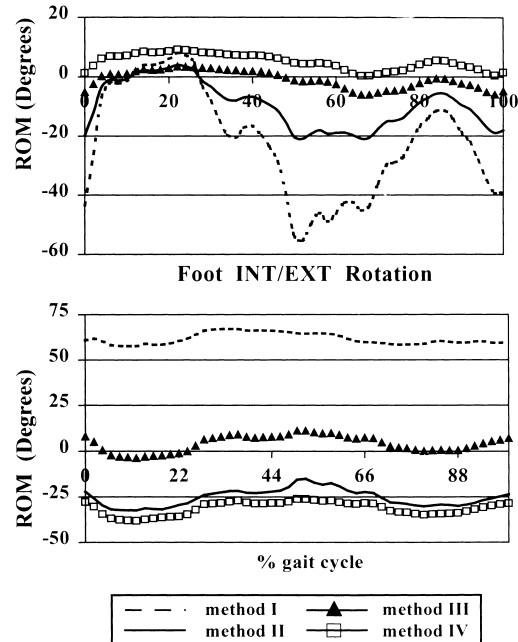


FIG. 6. Clinical subject with 90° external tibial torsion. Ankle plantarflexion–dorsiflexion motion of the right foot and transverse plane foot rotation motion of the right limb of a single gait cycle processed with methods 1–4.

onset of push-off after gastrocnemius fascia lengthenings. They concluded that in their series of 20 cerebral palsy patients who underwent a modified version of the Baker lengthening, improvement was seen in their dynamic ankle motion, which resulted in enhanced ankle power at push-off. Segal et al. (17) reported a series in which gait analysis was used as a tool to define calcaneal gait patterns in children with spastic diplegia after heel cord lengthening. In this series, a 4° increase in dorsiflexion from a previously reported normal range during midstance indicated calcaneal gait. Recent outcome studies looking at the efficacy of surgery or of botulinum toxin for treating equinus gait patterns have relied heav-

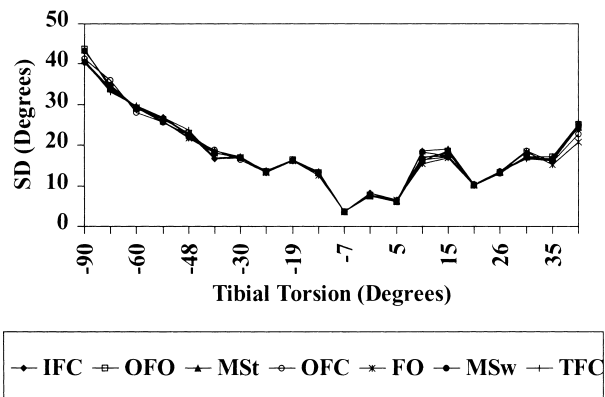


FIG. 7. Standard deviation of methods 1–4 for the transverse plane foot rotation motion versus the tibial torsion value at seven key points in the gait cycle: initial foot contact (IFC), opposite foot off (OFO), midstance (MSt), opposite foot contact (OFC), foot off (FO), midswing (MSw), and terminal foot contact (TFC).

**TABLE 2.** Pearson correlation of the standard deviation of the seven key points in the gait cycle versus tibial torsion for ankle PF/DF and foot rotation

Key point in gait cycle	Ankle PF/DF tibial torsion (90°–0°) ext.	Tibial torsion (0°–39°) int.	Foot rotation tibial torsion (90°–0°) ext.	Tibial torsion (0°–39°) int.
Initial foot contact	0.90	0.72	0.97	0.73
Opposite foot off	0.70	0.81	0.97	0.76
Midstance	0.84	0.67	0.98	0.70
Opposite foot contact	0.79	0.58	0.97	0.71
Foot off	0.92	0.61	0.97	0.75
Midswing	0.94	0.63	0.97	0.75
Terminal foot contact	0.88	0.68	0.97	0.73

PF/DF, plantarflexion–dorsiflexion.

ily on small documented changes in ankle range of motion in the sagittal plane (20).

In this study, we found that processing of the same kinematic data by the four methods available in VCM software led to large differences in the calculated ankle PF/DF and transverse plane ankle rotation for patients with tibial torsion abnormalities commonly found in children with cerebral palsy. The deviations are large enough to bring into question the significance of observed differences between treatment methods for ankle equinus if the same modeling assumptions are not being used for data interpretation by different centers or by the same center when looking at pre- and posttreatment studies. We found that for tibial torsion >20° external or >15° internal, the resultant dynamic ankle PF/DF data differed by >5° as a function of the calculation method alone. Larger torsional abnormalities resulted in kinematic differences of >10°.

In most anatomic models used for motion analysis, it is generally assumed that each segment is a rigid body. This assumption is valid for most segments but is problematic when evaluating the multiple bones and joints of the foot. Complex models incorporating 4–8 rigid segments in the foot have been described (1,2,11,15,16), but these models require 12–16 surface markers on the foot and shank segments to more accurately measure all the functional joints in the foot. A more simplistic model of the foot has been used by many centers as a solution to the critical problem of accurately and reproducibly tracking limited number of markers on very small feet. VCM allows the user to model three rotational degrees of freedom about 3 anatomic axes (flexion/extension, adduction/abduction, internal/external) for the pelvis, hips, and knees. It allows 2 rotational degrees of freedom (flexion/extension and internal/external rotation) for the ankle complex (3,9,12). This allows users to derive the motion of the ankle complex using 4 different processing methods, allowing the end user to choose the method most appropriate for the population being evaluated.

We have found the simplicity and flexibility of the VCM model to be advantageous when testing children with severe musculoskeletal deformities. Although VCM software was used for the data analysis in this study, we believe the results from this calculation method com-

parison will be present in other commercially available software packages that use comparable modeling. The four methods for the foot and ankle modeling in VCM yielded comparable kinematic data only when the clinical measure for tibial torsion remained within a normal range (18). Similar findings were reported by Kaufman et al. (10). They determined tibial torsion from computed tomographic scan measurements and found a significant correlation with the calculated value derived from surface markers in a normal population. To the best of our knowledge, no similar studies have been done for patients with significant musculoskeletal abnormalities.

As a result of this study, we have chosen to use method 4 when using VCM software for the evaluation of children with cerebral palsy. We found that method 4 most consistently agreed with our clinical observations of PF/DF. In method 4, the Grood and Suntay (8) convention for joint articulation is not applied, as is the case in the first 3 methods. Plantarflexion or dorsiflexion is indicated when the forefoot or toe marker moves downward or upward past the ankle PF/DF plane, which intersects the virtual ankle joint center during the gait cycle. In addition, this method quantifies ankle rotation as internal or external based on the orientation of the foot relative to the knee flexion axis. This method is still a simplified model of the foot and ankle motion compared with the true anatomy. Caution is warranted when interpreting patients with severe midfoot break because VCM models the foot as a rigid body. However, with a clear understanding of the model and its limitations, we have obtained clinically useful information about our various clinical populations.

In summary, patients with clinically significant torsional malalignment may manifest kinematic changes in their gait that can result from data processing alone and may not represent true clinical changes. Gait studies of patients with these clinical abnormalities need to be interpreted cautiously to ensure that the data processing is consistent in the pre- and posttreatment studies and between centers. We believe that changes recorded by any center that is consistent in their conventions will reflect true change. The magnitude of that change, however, may be altered by the modeling assumptions of the software used for the analysis.

**Acknowledgments:** The authors thank Frank L. Buczek, Ph.D., for technical oversight, Richard Browne, Ph.D., for statistical advice and editorial review, and Janet Fein for editorial assistance.

## REFERENCES

1. Abu-Faraj ZO, Sampath G, Smith PA, et al. A clinical system for analysis of pediatric foot and ankle motion. *Gait Posture* 1997;5:149.
2. Abuzzahab FS, Harris GF, Kidder MS. A kinetic model of the foot and ankle. *Gait Posture* 1997;5:148.
3. Bell AL, Pederson DR, Brand RA. A comparison of the accuracy of several hip center location prediction methods. *J Biomech* 1990;23:617-21.
4. Davis RB, Ounpuu S, Tyburski D, Gage JR. A gait analysis data collection and reduction technique. *Hum Movement Sci* 1991;10:575-87.
5. Gage JR. Gait analysis for decision-making in cerebral palsy. *Bull Hosp Jt Dis* 1983;43:147-63.
6. Gage JR. *Gait analysis in cerebral palsy*. London: MacKeith Press, 1991:118-200.
7. Gage JR, Ounpuu S. Gait analysis in clinical practice. *Semin Orthop* 1989;4:72-87.
8. Grood ES, Suntay WJ. A joint coordinate system for the clinical description of three-dimensional motions: application to the knee. *J Biomech Engineer* 1983;105:136-44.
9. Kadaba MP, Ramakrishnan HD, Wootten ME. Measurement of lower extremity kinematics during level walking. *J Orthop Res* 1990;8:383-92.
10. Kaufman KR, Moitoza JR, Sutherland DH. *Relation between external markers and tibial rotation measurements*. Presented at the International Symposium on Three-Dimensional Analysis of Human Movement, Montreal, 1991.
11. Kidder SM, Abuzzahab FS, Harris GF, Johnson JE. A system for the analysis of foot and ankle kinematics during gait. *IEEE Trans Rehab Engineer* 1996;4:25-32.
12. Oxford Metrics. *VICON Clinical Manager user's manual*. Oxford: Oxford Metrics Ltd., 1995.
13. Perry J. *Gait analysis: normal and pathological function*. Thorofare, NJ: Slack Inc., 1992:169-281.
14. Rose SA, DeLuca PA, Davis RB, et al. Kinematic and kinetic evaluation of the ankle after lengthening of the gastrocnemius fascia in children with cerebral palsy. *J Pediatr Orthop* 1993;13:727-32.
15. Scott SH, Winter DA. Talocrural and talocalcaneal joint kinematics and kinetics during the stance phase of walking. *J Biomech* 1991;24:743-52.
16. Scott SH, Winter DA. Biomechanical model of the human foot: kinematics and kinetics during the stance phase of walking. *J Biomech* 1993;26:1091-104.
17. Segal LS, Thomas SE, Mazur JM, Mauterer M. Calcaneal gait in spastic diplegia after heelcord lengthening: a study with gait analysis. *J Pediatr Orthop* 1989;9:697-701.
18. Staheli LT, Engel GM. Tibial torsion: a method of assessment and a survey of normal children. *Clin Orthop* 1972;86:183-6.
19. Sutherland DH, Hagy JL. Measurement of gait movements from motion picture film. *J Bone Joint Surg Am* 1972;54:787-807.
20. Sutherland DH, Kaufman KR, Wyatt MP, et al. Double-blind study of botulinum A toxin injections into the gastrocnemius muscle in patients with cerebral palsy. *Gait Posture* 1999;10:1-9.
21. Sutherland DH, Olshen RA, Biden EN, Wyatt MP. *The development of mature walking*. London: MacKeith Press, 1988:188-205.
22. Winters TF, Gage JR, Hicks R. Gait patterns in spastic hemiplegia in children and young adults. *J Bone Joint Surg Am* 1987;69:437-41.